Development and Evaluation of a Novel Intranasal Spray for the Delivery of Amantadine

Journal Item

Development and evaluation of a novel intranasal spray for the delivery of amantadine

S. Lungare [a], J. Bowen [b,c], R.K.S. Badhan [d *]

[a] Aston University, School of Life and Health Sciences, Birmingham, B4 7ET, UK;
[b] The Open University, Department of Engineering and Innovation, Milton Keynes, MK7 6AA, UK;
[c] University of Birmingham, School of Chemical Engineering, Birmingham, B15 2TT, UK;
[d] Aston University, Aston Research Centre for Healthy Ageing, Life and Health Sciences, Birmingham, B4 7ET, UK;

[*] Corresponding author
Dr Raj K. S. Badhan
School of Life and Health Sciences
Aston University
Birmingham
B4 7ET
Telephone: +44 121 204 3288
Email: r.k.s.badhan@aston.ac.uk

ABSTRACT

The aim of this study was to develop and characterise an intranasal delivery system for amantadine (AMT). Optimal formulations (F) consisted of a thermosensitive polymer Pluronic® 127 (P127) and either carboxy methyl cellulose (CMC) or chitosan (CS) which demonstrated gel-transition at nasal cavity temperatures (34 °C ± 1 °C). Rheologically, the loss tangent (Tan δ) confirmed a three-stage gelation phenomena at 34 °C ± 1 °C and non-Newtonian behaviour. Storage of FCMC and FCS at 4 °C for 8 weeks resulted in repeatable release profiles at 34 °C when sampled, with a Fickian mechanism earlier on but moving towards anomalous transport by week 8. Polymers (P127, CMC and CS) demonstrated no significant cellular toxicity to human nasal epithelial cells up to 4 mg/mL and up to 1 mM for AMT (IC50: 4.5 mM ± 0.05 mM). FCMC and FCS demonstrated slower release across an *in-vitro* human nasal airway model (43-44 % *vs* 79 % ± 4.58 % for AMT). Using a human nasal cast model, deposition into the olfactory regions (potential nose-to-brain) was demonstrated upon nozzle insertion (5 mm) whereas tilting of the head forward (15°) resulted in greater deposition in the bulk of the nasal cavity.

KEYWORDS

Parkinson's disease; rheology; nasal; RPMI 2650; nose to brain; thermoresponsive;

INTRODUCTION

Parkinson's disease (PD) is an ageing associated progressive neurological disorder and affects 1.5 % of the population over 65-years of age [1], with age-adjusted prevalence rates thought to be around 150 per 100,000 with a suggested mean onset in the 70's [1]. Ageing is the largest single risk factor for the development of PD and the pathogenesis of PD is composed of a range of events leading towards neuronal apoptosis, primarily of degradation of dopamine neurones in the *sustantia nigra*. The mainstay of clinical drug therapy focuses on increases the levels of dopamine (DA) in the brain, with oral dosing of levodopa being the most commonly used to pharmacological intervention treatment to reverse the symptoms of PD. It is also common to use adjunct therapies in conjunction with levodopa, such as the weak NMDA-type receptor antagonist amantadine, which can aid in blocking dopamine reuptake.

One of the major complications of PD is the emergence of dysphagia affecting the ability to ingest/swallow and is a thought to affect between 45-95 % of PD patients [1,2] and has significant implications for orally dosed therapeutics such as amantadine and other anti-Parkinsonian therapeutics agents. Furthermore the occurrence of bradykinesia and morning akinesia is often associated with delayed gastric emptying following the oral administration of anti-Parkinsonian therapeutics. This is again confounded by the use of dopaminergic and other concomitant meditation interventions. At least 24% of PD patients are thought to suffer from gastroparesis, the delay in empting of the stomach, which will inevitably impact upon clinical outcome of any orally administered medication. A more recent approach for therapeutic delivery is through the intranasal route to obtain systemic deposition as a practical alternative to oral and parenteral routes [3,4].

The primary function of the nasal cavity is respiration and olfaction. The nasal cavity (in humans) is divided in to two symmetrical halves by a septum with each cavity sub-dived into four areas namely vestibules, atrium, respiratory region and olfactory regions. With a surface area of 150 cm^2, total volume of 15-20 mL the nasal cavity provides an optimal absorption area for drugs into the systemic circulations which would inevitably enhance the bioavailability of the therapeutic agent, particularly those which demonstrate poor oral absorption (intestinal permeation) or significant first-pass metabolism (extra-hepatic and hepatic) [5,6]. Although originally exploited for the delivery of locally acting agents (allergic of infections rhinitis, nasal pluposos and sinusitis) the highly vascularised nature of the nasal cavity has provided a portal for systemic delivery of small molecules and biomolecules [7]. The nasal cavity can provide larger surface area for rapid systemic absorption due to its highly vascularised surface [8]. This non-invasive route not only provides rapid onset of action, but often increased bioavailability in low doses as it bypasses the first pass metabolism [9].

Although intranasal drug delivery offers many advantages, one of the main limitations is the short residence time of the formulation in the nasal cavity, as a result of mucociliary clearance (MCC) [10]. This movement involves the beating of mucocilia at a frequency of 1,000 strokes per minute and hence movement of mucus of 5 mm/minute [11]. Thus the clearance of any nasally administered formulation further back towards to the nasopharynx is often a limiting factor in clinical administration and results in a short nasal residency half-life of 15-20 minutes [12].

An ideal formulation would be one that was capable of prolonging residence time within the nasal cavity and therefore enhance the bioavailability of the drug. To achieve this goal, the use of intelligent polymer based systems have now become more commonplace in this field and particularly the use of responsive systems which may respond to the nasal cavity temperature [13-22] or pH [23-27] have increased amongst researchers. Furthermore, the use of mucoadhesive polymers [4,27-33] to enhance the adhesion of the formulations onto the nasal mucosa has further demonstrated the ability to prolong contact time with the mucosa and hence increase bioavailability [10,15,18,23,34-36].

The primary aim of this study was to develop an intranasal thermoresponsive hydrogel based delivery system for the delivery of anti-Parkinson's drugs, using amantadine as a model candidate drug. The study objectives were to utilise thermoresponsive polymers, for example Pluronic F127 (P127) [13], mucoadhesive polymers (carboxymethyl cellulose and chitosan) and surfactant (PEG4000 and PEG 12000) to aid and enhance formulation delivery and

retention within the nasal cavity using a multi-dose nasal spray and human nasal cast. In order to develop and assess the formulations a range of studies were conducted and included rheological, stability, biological compatibility and nasal targeting of the formulations.

METHODS

Materials

Eagle's Minimum Essential Medium (MEM), Dulbecco's phosphate buffered saline (PBS), L-glutamine 200 mM, non-essential amino acids (NEAA), penicillin/streptomycin and trypsin-EDTA solution were obtained from PAA Laboratories (Austria); fetal bovine serum (FBS) (Labtech Intl Ltd. East Essex, UK); polyethylene glycol 4000 (PEG4000), polyethylene glycol 12000 (PEG12000), chitosan-medium molecular weight (CS), sodium chloride, potassium chloride, magnesium sulphate, calcium chloride, acetonitrile, orthophosphoric acid, acetic acid, ethanol, sodium hydroxide, potassium chloride and sodium chloride were obtained from Fisher Scientific (Loughborough, UK); gentamycin, (3-(4, 5-dimethylthiazol-2-yl)-2, 5-diphenyl tetrazolium bromide) MTT, Trypan blue dye, Pluronic® F127 (P127), sodium carboxymethyl cellulose (CMC), amantadine hydrochloride (AMT), sodium metabisulphate, mucin from porcine stomach, boric acid, dimethyl sulfoxide (DMSO) and benzalkonium chloride were obtained from Sigma-Aldrich (St. Louis, MO, USA).

Formulation development

Formulations were initially prepared by a modified 'Cold method' approach as originally described by Schmolka (1973) [13]. Briefly fixed quantities of excipients were utilised in all formulations and consisted of d-sorbitol (humectant) (0.5 % w/v), sodium metabisulphate (antioxidant) (0.1 % w/v) and benzalkonium chloride (surfactant) (0.1 % w/v). Additional polymers were incorporated and included mucoadhesives (CMC and CS) and permeation enhancers[37]/modulators of gelation temperature[14,38] (PEG4000 and PEG 12000) at concentrations between 0.5-1.5 % w/v. These components were combined with ultrapure water under constant stirring. This was followed by AMT (0.5-1.5 % w/v) and the resulting solution was kept in an ice bath for 2 hours prior to the dropwise of P127 (15-20 %) and storage at 4 °C for 12 hours. Prior to use, the pH of all formulations were adjusted to 5.5[16,39]. Formulations were developed according to variation in the concentration of P127, mucoadhesive polymer, and drug content.

Sol-gel transition ($T_{sol\text{-}gel}$)

A modified method described by Zaki *et al.* [8] was used to determine the sol-gel transition temperature ($T_{sol\text{-}gel}$). A sample of each formulation (1 g) was transferred to a glass vial and heated in a dry block (Techne Dri-Block ® DB-2D), initiated at 20 °C and increased by 1 °C after every 5 minutes of equilibration time. The $T_{sol\text{-}gel}$ point was defined as the temperature whereby the upper meniscus of the gel did not move upon tilting the vial by 90 ° and this was used to demark optimal formulations. The optimal subset of formulations were then further characterised.

Rheological characterisation

To assess the rheological properties of the formulations, rheological measurements were carried out on AR-G2 Rheometer (TA Instruments, USA), using parallel plate geometry with 40 mm steel plates having a gap 1.0 mm. The approximate sample volume used was 1.26 mL and the instrument was used in the oscillatory mode in the linear viscoelastic range of the sample. Steady state behavior was assessed at ambient (18 °C) and nasal (34 °C) temperatures over a shear rate range from 0.1 to 100 s^{-1}.

To quantify the rheological properties, the Ostwald-de Waele relationship (often called the power law) was applied to relate the shear stress (σ) is related to a consistency coefficient (k), the shear rate ($\dot{\gamma}$) and an index value (n):

$$\sigma = k\dot{\gamma}^n$$

which is applicable to the formulations in light of the constant shear viscosity curves. In the context of rheology, the index value can be used to determine the type behavioural flow, with Newtonian behaviour when $n = 1$. When the magnitude of n is < 1, the underlying rheological process is shear-thinning (pseudoplastic flow) and then when $n > 1$ the fluid is shear-thickening.

***In-vitro* mucoadhesion**

The method of Nakamura *et al.* (1996) [24] was adapted to measure the mucoadhesion of the formulation systems. Briefly, 100 g of a hot 1 % agar and 2 % mucin mixture in PBS (pH 6.0) was cast onto a glass plate and left to gel at 4 °C for 12 hours. The gel plate was then equilibrated at 34 °C for 1 hour followed by the application of a 250 µL sample of each formulation when the plate was kept at a 45° angle at 34 °C. This process was repeated using a 1 % agar mixture (without mucin) and the mucoadhesion of the formulations were calculated by a 'displacement' value (measured in cm) reflecting the difference in gel movement in the presence and absence of 2 % mucin.

AMT derivatisation and HPLC detection

To quantify the release of AMT from the formulations, a pre-column derivatisation method for memantine was modified in order to enable detection of AMT [40]. Briefly, to 50 µL of sample or standard solution of AMT, 40 µL of 0.015 M FMOC and 50 µL of 0.5 M borate buffer were added and kept at room temperature for 20 minutes prior to the addition of 360 µL of a 0.05M borate buffer:acetonitrile (50:50 v/v) diluent. A Shimadzu HPLC system was used with a Phenomenex Luna C18 (150 × 4.6 mm) 5 µm column. The mobile phase consisted of phosphate buffer:acetonitrile (20:80 v/v). The column was maintained at 30 °C and 10 µL injected. The flow rate was maintained at 2 mL/minute with run time of 7 minutes. The UV detection of derivatised AMT was measured at 265 nm. The intra/inter-day precision was determined and the limit of detection (LOD) and limit of quantitation (LOQ) were calibrated according to ICH (QR (R1)) recommendations [41].

Stability assessment

Optimised formulations were stored in stability cabinets maintained at 4 ± 1 °C (Sanyo Medicool, UK) and 25 ± 2 °C (Firlabo, France) at a humidity of 60 % ± 5 %. The stability of the formulation was assessed based on the gelation of a sample of the formulation at 34 °C within 5 minutes, followed by assessment of the extent of drug release.

The release of AMT from the formulations were assessed by a 'membrane-less' diffusion system [20,42,43]. A mass of formulation (0.25 g) appropriate for the nasal cavity volume was transferred to a glass vial and allowed to equilibrate in a dry block at 34 °C. Artificial nasal electrolyte (ANE) (0.8 g/L NaCl, 3 g/L KCl, and 0.45 g/L $CaCl_2$, pH 6.8) [44] was used as release media and 100 µL transferred onto the gelled formulation. This volume was completely withdraw and replaced with fresh ANE at each time point. Samples were analysed by a pre-column derivatisation method followed by HPLC analysis.

***In-vitro* drug release kinetics**

Several kinetic drug release mathematical models were used to assess drug release from the formulations. The best-fit to the mathematical models described below confirmed the appropriate release kinetics:

Higuchi model: $\frac{M_t}{M_\infty} = kH \cdot t^{\frac{1}{2}}$

where M_t/M_∞ is the drug fraction released at time *t* and *kH* is the Higuchi constant.

Zero order model: $\frac{M_t}{M_\infty} = k_0 \cdot \mathrm{t}$

where M_t/M_∞ is the drug fraction released at time *t* and k_0 is the zero-order release constant.

First order model: $\frac{M_t}{M_\infty} = 1 - e^{-k_1 t}$

where M_t/M_∞ is the drug fraction released at time *t* and k_1 is the first-order release constant.

Power law: $\frac{M_t}{M_\infty} = kKP \cdot t^n$

where M_t/M_∞ is the drug fraction released at time *t*, *kKP* is a kinetic constant which describes the structural and geometrical elements of the formulations and *n* is the release exponents which is used to indicate the mechanism of drug release. The power law, otherwise known as the Korsmeyer-Peppas power law [45], has been used in many pharmaceutical formulations [46-49]. The value of *n* is important in understanding the mechanism of release when it is unknown and often polymeric formulations can be categorised accordingly to this scale. When $n \leq 0.45$ drug release is diffusion controlled and sometimes referred to as Fickian diffusion and when $n > 0.89$ the diffusion is indicative of erosion controlled drug release or class-II kinetics. For situations where $0.45 < n \leq 0.89$

the diffusion is a complex mixture of both processes and often termed anomalous transport. In all cases this is based on the assumption of release from a cylinder and applied to cumulative release rates < 60 % [45].

Human nasal epithelial cell culture model

The immortalised human nasal epithelial cell line RPMI 2650, was used to assess the compatibility of the formulations with human nasal epithelia and to develop an *in-vitro* nasal epithelial cell culture model [50] to assess drug release/transport. Cells were grown in MEM supplemented with 10 % FBS, 1 % L-glutamine, 1 % NEAA, 1% penicillin-G/streptomycin in a humidified 37 °C incubator with 5 % (v/v) CO_2 [51]. The media was changed every 2 days.

(3-(4,5-Dimethylthiazol-2-yl)-2,5-Diphenyltetrazolium Bromide) (MTT) assay

To assess cellular toxicity, RPMI 2650 cells were seeded at a density of $4x10^4$ cells per well of a 96-well plate and allowed to attach for 24 hours. The media was removed and replaced with 200 µL of media containing either AMT (0.01-50,000 µM), mucoadhesive polymers or P127 (10-4000 µg/mL) and incubated for 24 hours at 37 °C in a 5 % (v/v) CO_2 humidified air environment. Subsequently 20 µL of 5 mg/mL MTT dissolved in PBS was added to each well and incubated at 37 °C in a humidified air environment for 4 hours. After incubation the medium was removed and 100 µL of DMSO was added and the plates left to incubate for 15 minutes in the dark. The UV-absorbance of the formazan product was determined at 595 nm. Each concentration was assayed in eight wells and run in three independent experiments and results expressed as percentage cytotoxicity relative to a control (0.5% DMSO).

Human nasal epitheial airway cell culture model: AMT transport

To assess the release and transport of AMT from formulations, an *in-vitro* nasal epithelial airway cell culture model was developed with RPMI 2650 cells seeded onto collagen-coated 6-well permeable inserts (ThinCerts™) at a seeding density of $4x10^5$ cells/cm^2 [52] [50] and grown for 14 days. On days 10-14 an air-liquid interface (ALI) was initiated with the removal of apical media. The integrity of the monolayer was determined by measuring the trans-epithelial electrical resistance (TEER) using an EVOM epithelial voltohmmeter (World Precision Instruments Inc.). Inserts were deemed acceptable where the TEER value was above 180 Ω.cm^2 [52] [50].

Immediately prior to the start of the transport study, maintenance media was replaced with transport media (HBSS with 25 mM HEPES) and the cells left to acclimatise for 30 minutes in a humidified 37 °C incubator with 5% (v/v) CO_2. A 1 mL sample of formulation was placed into the apical chamber, after removal of transport media from apical and basolateral compartment, and returned to the incubator for 5 minutes. Once gelled, fresh transport media was placed into the basolateral chamber and 250 µL samples withdrawn at 5, 15, 30, 60, 120, 150 and 180 minutes and replaced with fresh pre-warmed media. Withdrawn samples were derivatised and AMT release quantified by HPLC analysis.

Nasal spray systems: droplet size distribution

To assess the potential *in-vivo* deposition characteristics of the proposed nasal formulation, a multi-dose pump spray delivery system was employed to characterise the formulation droplet size distribution using a laser diffraction technique. The HELOS (Sympatec, UK) system was used with an R3 lens (measuring range 0.5-175 µm). The nasal pump was vertically mounted 3 cm away from the laser path and a vacuum source was mounted anterior to the pump system. The pump systems were pre-actuated prior to mounting, and actuated three times to detect the particle size distribution. Data was reported as volume diameters at 10 %, 50 % and 90 % of the cumulative undersized volumes. Span was calculated as: [(Dv90-Dv10)/Dv50].

Nasal spray system: human nasal cast deposition

To assess the potential *in-vivo* deposition characteristics of the proposed nasal formulation, a multi-dose pump spray delivery system was employed to assess the deposition of formulations into an anatomically correct human nasal cast model (Koken Ltd, Japan). The inner surface of each nostril was evenly coated in a water-indicated dye (Kolor Kut, USA). Formulations were loaded into the spray pump, pre-actuated, before one actuation was

delivered into the nasal cast where the cast was fixed in an upright head position. The impact of spray angle and nostril insertion depth on nasal deposition was analysed through photographing colour changes. The captured images were subsequently processed through pixel quantification software to quantify the deposition patterns and calculate the deposition surface area [53]. The depositions of within the nasal cast was classified according to the predominate regions of deposition within the cast, i.e. lower nasal regions (nasal vestibule), the middle/upper nasal regions (turbinates) and the olfactory regions were assessed.

Statistical analysis

Unless otherwise stated, three independent experiments were carried out for each study. Statistical significance was evaluated by one-way ANOVA or paired two-tail Students t-test using GraphPad Prism version 6.00 for Windows (GraphPad Software, La Jolla California USA, www.graphpad.com). Calculations of IC50 were determined using a four-parameter logistic sigmoidal fitting function within GraphPad Prism. Unless otherwise states, data is reported as mean ± standard deviation (SD). A significance level (p-value) of < 0.05 was considered as statistically significant.

RESULTS AND DISCUSSION

The treatment of age-associated degenerative CNS disorders such as Parkinson's diseases, poses particular difficulties in the design of appropriate drug delivery systems capable of overcoming the hindrances associated with dyskinesia and dystonia that are inherent in current pharmacological interventions for PD. Although reformulation of existing orally dosed formulations may provide some benefit there is an inherent need to provide an alternative delivery routes of a range of CNS disorders which can both provide ease of clinical use but also improve the bioavailability of the therapeutic.

The nasal mucosa fulfils this purpose in light of the large and vascularised route of access for drugs to the systemic circulation and can provide a relatively non-invasive approach to delivery drugs.

A key concern of any nasal administered formulation is the residency of the formulation within the nasal cavity. Existing formulations are often associated with a nasal drip or 'run-off' effect which potentially diminish the bioavailability of nasal formation. A novel development in this area has been the formulation of intelligent response based hydrogel nasal formulations which act to enhance residency within the nasal cavity [13-27].

Sol-gel transition ($T_{sol-gel}$)

The initial screening and optimisation resulting in 32 formulations, of which 3 demonstrated optimal gelation at the nasal cavity temperature of 34 °C ± 1°C [54]. These formulations were identified as FCMC (1 % w/v CMC), FPEG (1 % w/v PEG4000) and FCS (0.1 % w/v chitosan) and which all contained 17 % w/v P172 and 1% w/v amantadine (in addition to excipients).

Rheological behaviour

When assessing the properties of thermoresponsive gel-like systems, the storage/elasticity modulus (G') and the loss modulus (G'') are key metrics to describing the rheology of the formulation. The elasticity modulus is an important metric in this regard and measures the energy stored and which is subsequently recovered for each cycle of deformation [55]. It presents with lower values with reduced temperatures but significantly increases with an increase in temperature, and the point at which G' overtakes G'' indicates the initiation of the gelation phenomena. To assess this phase transition the ratio of G'' and G' (the loss tangent, Tan δ) was used, and where a phase-transition occurs an abrupt change in Tan δ is observed with values of < 1 indicating a greater G' compared to G'', indicative of gel formation. This phase transition is often associated with three distinct phases: (i) an initial stable liquid phase plateau at low temperatures; (ii) an abrupt transition phase during the gelation process; (iii) a late stage stable gel plateau.

All formulation demonstrated a gelation phenomenon, which initiated at approximately 26-28 °C, and was preceded by the stable plateau region (Figure 1). FCS and FCMC (Figure 1A) demonstrated a complete profile with three distinct phases culminating in a stable gel formulation, whereas FPEG (Figure 1A) only demonstrated two phases, plateau followed by a partial gelation phase, but did not form a stable a gel at the termination of the study (34 °C).

The rate of gelation is also a key determinant of residency within the nasal cavity and this was assessed through a time-sweep analysis at a fixed temperature (34 °C). FCMC demonstrated the quickest gelation of 28 ± 2 seconds which was followed by FCS (37 ± 3 seconds) and FPEG (68.5 seconds) (Figure 1B).

At nasal cavity temperatures, a significant shear thinning behaviour was observed in all formulations, indicative of temperature-induced gel formation when compared to ambient temperatures (Figure 2), with viscosities for 34 °C being statistically significantly different to those at 18 °C ($P < 0.0001$). Furthermore, at 34 °C no significant difference in viscosity was reported over the shear rate studied ($p = 0.227$), however FPEG demonstrated a statistically significant lower viscosity compared to FCS and FCMC ($P < 0.01$).

As the shear rate increased from 0.091 to 100 s^{-1}, the viscosity of the formulations dropped by 990-fold (FCMC), 409-fold (FCS) and 207-fold (FPEG) (Figure 2). However, all formulations exhibited non-Newtonian behaviour at nasal temperatures compared to Newtonian behaviour at ambient temperatures (Table 1).

From an interpretation of the Ostwald model, the gel structure can be changed as a result of any deformation induced changes in the gel particles, through changes in the alignment of the polymer chains and also any changes in the interactions between polymer chain segments and any side chains. Therefore, upon heating the values of *n* will be lower in for stronger gels due to an increase in the noncovalent forces of between neighbouring particles [56].

It was also apparent that the presence of different mucoadhesives can significantly alter the behaviour of the formulations. For examples, the viscosity of FCMC was always higher than all other formulations, and particularly at 34 °C where there is an approximate 8-fold difference between FCMC and FPEG. Furthermore, the FCMC demonstrated a much lower *n*-value compared to FCS and FPEG (Table 1), suggesting a stronger gel formation at 34 °C. This phase represents the gradual conversion into a highly viscous/solid state. During this phase the intricate hydrogen-binding network between the unimers of F127 and water molecules are disrupted and drives the formation of micelles, which further aggregate to form the physical gel-like structure. [57]. On the basis of ^{13}C NMR studies Pisal [58] suggested that at high temperature, conformational changes in the methyl group of the polyoxypropylene within the hydrophilic micellar region and in the motion of the hydrophilic end chains takes place. This results in dehydration and end chain friction, which causes the gelation.

***In-vitro* mucoadhesion**

Mucoadhesion is defined as a state where at least one biological material is held with another material for a prolonged period of time [59]. In the context of drug delivery, this can be defined as the adhesion of an artificial material (such as a polymer system) to a biological substrate material [60]. We assessed the mucoadhesion of optimized formulations using an inclined-plate method in the presence and absence of mucin [24], with mucoadhesion assumed to have occurred if the displacement of the formulation in the absence of mucin is greater than in the presence of mucin.

The displacement transfer test demonstrated that all formulations showed a statistically significant ($P \leq 0.001$) displacement in the absence of mucin (Figure 3). The difference between the absence and presence of mucin is indicative of the displacement effect and FCMC demonstrated the least extent of displacement (2.26 cm) with FPEG demonstrating the greatest extent of displacement (3.8 cm).

The superiority of FCMC and FCS, compared to FPEG, is presumed to be a function of the enhanced rheological properties FCMC and FCS possess (Figure 1 and 2). The fact that displacement is observed in the absence of mucin would indicated that the use of is able to recover some of the mucoadhesive properties of the mucoadhesive polymers included within the formations, and although known to show less biophysical properties as compared to native mucin, this purified mucin has less batch-to-batch variation and hence provides better reproducibility in measuring mucoadhesive force [61].

AMT derivatisation and HPLC detection

The HPLC was successfully able to detect the derivatisation of AMT with a retention time of 4.4 minutes. Percentage RSD for system precision (0.120 %) and method precision (0.121 %) were within the acceptable limits of 1 % and 2 % respectively.

The linearity response of amantadine was determined using concentrations ranging from 0.0078 to 1.0 mg/mL and the response was linear over the specified range with a correlation coefficient of 0.9998, a slope of 1385904 ± 33080 and an intercept of -13515 ± 1045. The validity was verified by ANOVA with no deviation from linearity.

Stability assessment

To assess the stability of the optimised formulations, batches were prepared and stored in stability cabinets at 25 °C/60 % RH and 4 °C for 8 weeks, with sampling at weekly intervals followed by assessment of AMT release conducted at nasal temperatures (34 °C). A prerequisite for conducting release studies was the successful gelation of the stability samples prior to initiation of release studies.

All formulations stored at 4 °C demonstrated successful sol-gel transition prior to the initiation of the release studies, confirming the thermoresponsive nature of the gel systems was maintained during the stability study duration. However only FCS demonstrated successful sol-gel transition when stored at 25 °C/60 % RH for 2 weeks, confirming that storage of formulations would be more appropriate at 'refrigerated' conditions to ensure stability of the products.

The cumulative percentage release at preparation and after 1 week storage at 4 °C were not significantly different for all formulations, reaching 15-17 % release (Figure 4A). Following 8 weeks storage at 4 °C, the quantity of AMT released from FCMS (16.15 % ± 0.82 %) was not significantly different to that at week 0 (16.86 % ± 1.13 %) (Figure 4B), however at earlier time-points during the release study (30-120 minutes) significant differences ($p < 0.05$) in the AMT quantity released were apparent (Figure 4B). For FCS, the amount of AMT released following 8 weeks storage at 4 °C (18 % ± 0.99 %) was significantly ($p < 0.05$) greater than that at week 0 (15.32 % ± 0.30 %) (Figure 4B). Significant differences in the release profile were also apparent during the initial phases of the release study (30-60 minutes) (Figure 4B).

As the formulations presented are inherently based on 'swellable' type polymer systems, the diffusion was also modelled by the Korsmeyer-Peppas power law and generally demonstrated Fickian-type diffusion early on (except for FCS). By week 8 this had moved towards anomalous transport (Table 2), whereby drug diffusion and the polymer relaxation were contributing to the overall release kinetics.

The movement towards anomalous transport can be explained by considering the relationships between the two driving forces influences the diffusional process within the polymer system, namely the rate of solvent diffusion (R_D) and the rate at which polymer chains relax (R_R).

In Fickian-type diffusion (case-I), R_D is much slower compared R_R. For non-Fickian diffusion (case II, anaomolous and super case II) the main differences lies with the R_D whereby for case II $R_R >> R_D$, for anomalous-type kinetics $R_D \approx R_R$ and for super case II $R_D >> R_R$ [62-65]. Initially, formulations demonstrated Fickian-type diffusion (Table 2) but the Korsmeyer-Peppas exponent increased over the stability period to > 0.5 by week 8 moving towards anomalous transport (Table 2). This would suggest that polymer relaxation (swelling/erosion) plays a critical role in the release of AMT at earlier stability time points. The mathematical description and modelling of the casual factors for anomalous transport is challenging, and is beyond the scope of this study however a detailed review has been published discussing this issue [66].

The mass transport of AMT into the polymer network can be assumed to be comprised of 3 processes [67,68], whereby the solvent (water) is absorbed onto the surface of the polymer. The solvent molecules may then enter the lattice network of the polymer, which causes a 'swelling' of the network and elongation. This elongation is then counter balanced by an elastic-restrictive force to oppose the swelling. Eventually a state of equilibrium is reached when both forces are balanced, these process can significantly alter the kinetics of drug diffusion through the polymer network and are highly influenced by time-scale associated structural changes in the polymer [69-72]. The move towards anomalous transport over 8 weeks may suggest a polymer network time-associated affect [73,74], which becomes more apparent over the longer stability study. The equilibrium between swelling and elastic-restrictive force within the polymer may be associated with a time-dependent equilibrium, where equilibrium is not established immediately[75].

Although the formulations are in liquid-phase during the stability storage period, the interactions between both mucoadhesive polymers and thermoresponsive polymers may influence eventual formulations of the polymer networks, altering the equilibrium processes and hence contributing towards the anomalous transport.

Human nasal epithelial cell culture model: MTT assay

To investigate the toxicity of amantadine and polymers used within the formulations, a cellular viability study was conducted using the human nasal epithelial cell line RPMI 2650. Cell viability was generally maintained for AMT up to 1 mM, with an IC50 of 4.6 mM ± 0.05 mM (Figure 5A) when exposed for 24 hours. For all polymers tested, no significant decrease in cellular viability was observed up to 4 mg/mL (Figure 5B-D) and confirmed the formulations developed would be tolerable, from a cellular toxicity perspective, to human nasal epithelia. Furthermore, no previous reports have examined the *in vitro* toxicity profile of AMT towards human nasal epithelia and our reports demonstrated that 1 mM would be suitable for prolonged (up to 24 hours) exposure.

Human nasal epithelial airway cell culture model: AMT transport

The *in vitro* release of AMT alone and from formulations was further assessed in an *in vitro* nasal epithelial airway cell culture model over 3 hours (Figure 6).

In all formulations a statistically significant ($p \leq 0.01$) release of 43-44 % was observed over the duration of the transport study in comparison to that of AMT (79 % ± 3.58 %) (Figure 6). The mechanism of release, as described by the Korsmeyer-Peppas power law, was modelled according to a super case-II effect (n > 0.89) where the sorption of solvent results in breaking of the polymer network (termed solvent crazing) [76] as a result of the swelling of the gel within the vitreous nucleus and can be a result of crosslinking density [77], drug loading [78] and copolymer composition [79]. The super-case II diffusion of AMT from all gel systems was surprising, and therefore the release mechanism of AMT from the formulations is not clear as it is beyond the limits of the power law. It suggests that a rapid release of AMT occurred later in the experiment resulting in rapid relaxation governing/controlled transport of AMT from the polymer network [80 81]. The ionic composition of the media, comprising of a pH of 7.4, may have directly altered the state of ionisation within the polymer gel network, compared to the pH of the ANE (pH = 5.5) leading to an altered release profile, with the rapid release being a time-dependant reflection of the shift in equilibrium as the solvent (media) penetrates the polymer network [65,75].

Nasal spray systems: droplet size distribution

Prevention of pulmonary deposition of nasally administered spray formulations is paramount to ensure residency within the nasal cavity. Droplet size distribution is key in determining the potential for pulmonary deposition (< 2 µm) [82,83], however the droplet size is often dictated by the design of the orifice of the actuator device used to deliver the spray plume. For ensuring retention of drug within the nasal passages, droplet sizes of in-excess of 5 µm are recommended and represented our target cut-off [82,84].

Our formulations all demonstrated a diameter in excess of the traditional cut-off of 5 µm. (Table 3). FCS demonstrated a 10% fraction of 7.27 µm ± 0.28 µm (Table 3) closest to the cut-off for pulmonary deposition, whereas both FCMC and FPEG were above this. FCS also demonstrated the smallest diameter (VMD = 92.41 µm ± 1.72 µm). However, when considering the span of particle sizes, FCS was the broadest (0.96 ± 0.30) with both FCMC and FPEG showing a smaller distribution spread (Table 3). A one-way ANOVA confirmed droplet VMD were significantly different across all formulations ($p < 0.0001$), suggesting that the incorporation of different mucoadhesive polymers contributed to the differing polymer sizes with FCS demonstrating the small resulting droplets (92.41 µm ± 1.72 µm) and FCMC the largest (120.87 µm ± 0.59 µm). When considering the viscosity of the polymers used in each formulation (Figure 1), CMC resulted in the most viscous formulations and this may have contributed to the larger particle sizes, with similar trends observed for CS and PEG.

Nasal spray system: human nasal cast deposition

To assess the potential *in vivo* application of formulations, FCS and FCMC were taken forward to assess spray deposition within a human nasal cast model. The angle of spray administration was altered from 60-80° and the

impact on deposition patterns assed. For both formulations the administration angle had a significant effect on deposition, with an increased angle (80°) having a significantly pronounced localisation in the nasal vestibules and lower regions of the nasal cavity. For FCMC (Figure 7) this deposition area was significantly smaller greater than that for FCS (Figure 8).

Interestingly, spray angles of 60° and 70° lead to deposition of the formulation in the olfactory regions of the nasal cavity, suggesting the possibility for exploitation in nose-to-brain delivery of amantadine. FCS sprayed at an angle of 60° with insertion lead to olfactory deposition of 0.6-0.7 cm^2. For FCMC a greater olfactory deposition of 0.91 cm^2 was observed at 60° with insertion. Although the higher deposition for FCS may be a result of the smaller particle sizes for FCS (92.41 ± 1.72 µm) compared to 120.87 ± 0.59 µm, the impact of nozzle insertion for FCMC may enhance delivery onto the olfactory regions (Figure 7 and 8). When considering the surface area of the human olfactory mucosa (2-10 cm^2) [85], FCMC may be a viable candidate for further development targeting nose-to-brain drug delivery [86].

In both formulations, the impact of head position (15° forward) was important in governing nasal depositions, leading to significantly higher deposition within the middle-upper regions of the cast irrespective of the insertion angle.

The higher viscosity of FCMC compared to FCS resulted in significantly larger particle sizes ($p < 0.001$) for the optimal formulations and may have resulted in a more focussed (less disperse) spray plume resulting in more localised deposition patterns. In contrast, the lower viscosity of FCS, leading to small particles would lead to a wider plume and greater deposition in the nasal cavity [87,88].

As a viable vehicle for nasal or olfactory delivery and residency of formulations within the nasal cavity, the optimised formulations demonstrated rapid gelation (FCS: 36.6 s; FCMC: 28 s) (Figure 1) with minimal displacement within the nasal cavity (FCS 0.035 cm/s; FCMC: 0.038 cm/s) (Figure 3). When considering their potential residency within the nasal cavity, the sol-gel conversion and displacement would result in minimal nasal cavity displacement (FCS: 1.28 cm; FCMC: 1.06 cm). *In-vitro* release studies were conducted for 3-hours, with the gel structure intact following the release studies, hence the residence *in-vivo* would be expected to be at least 3-hours. Furthermore, the identification of potential nose-to-brain delivery, through olfactory deposition, would suggest that these formulations may be adapted to better exploit this 'direct' transfer route to the brain.

CONCLUSION

This study has investigated the potential to administer the anti-Parkinsonian drug amantadine through the nasal route using a mucoadhesive and thermoresponsive hydrogel formulation systems. We have demonstrated that both carboxymethyl cellulose and chitosan can provide the requirements for mucoadhesion in these formulations, whilst also leading to a relatively stable formulation which can be targeted to delivery drug in specific regions of the nasal cavity dependant on administration angle and nozzle insertion depth. Furthermore, our results have indicated the potential for nose-to-brain delivery of amantadine, yielding a potentially novel avenue therapeutics delivery route to avoid the blood-brain barrier.

REFERENCES

1. Foltynie T, Brayne CE, Robbins TW, Barker RA 2004. The cognitive ability of an incident cohort of Parkinson's patients in the UK. The CamPaIGN study. Brain : a journal of neurology 127(Pt 3):550-560.
2. Leopold NA, Kagel MC 1997. Pharyngo-esophageal dysphagia in Parkinson's disease. Dysphagia 12(1):11-18; discussion 19-20.
3. Leonard AK, Sileno AP, Brandt GC, Foerder CA, Quay SC, Costantino HR 2007. In vitro formulation optimization of intranasal galantamine leading to enhanced bioavailability and reduced emetic response in vivo. Int J Pharm 335(1-2):138-146.
4. Ikechukwu Ugwoke M, Kaufmann G, Verbeke N, Kinget R 2000. Intranasal bioavailability of apomorphine from carboxymethylcellulose-based drug delivery systems. International journal of pharmaceutics 202(1-2):125-131.
5. Bitter C, Suter-Zimmermann K, Surber C 2011. Nasal drug delivery in humans. Current problems in dermatology 40:20-35.
6. Illum L 2012. Nasal drug delivery - recent developments and future prospects. J Control Release 161(2):254-263.
7. Ozsoy Y, Gungor S, Cevher E 2009. Nasal delivery of high molecular weight drugs. Molecules 14(9):3754-3779.
8. Zaki NM, Awad GA, Mortada ND, Abd Elhady SS 2007. Enhanced bioavailability of metoclopramide HCl by intranasal administration of a mucoadhesive in situ gel with modulated rheological and mucociliary transport properties. European journal of pharmaceutical sciences : official journal of the European Federation for Pharmaceutical Sciences 32(4-5):296-307.
9. Pires A, Fortuna A, Alves G, Falcão A 2009. Intranasal drug delivery: how, why and what for? Journal of Pharmacy & Pharmaceutical Sciences 12(3):288-311.
10. Ugwoke MI, Verbeke N, Kinget R 2001. The biopharmaceutical aspects of nasal mucoadhesive drug delivery. The Journal of pharmacy and pharmacology 53(1):3-21.
11. Illum L 2002. Nasal drug delivery: new developments and strategies. Drug discovery today 7(23):1184-1189.
12. Vyas TK, Shahiwala A, Marathe S, Misra A 2005. Intranasal drug delivery for brain targeting. Current drug delivery 2(2):165-175.
13. Schmolka IR 1972. Artificial skin. I. Preparation and properties of pluronic F-127 gels for treatment of burns. J Biomed Mater Res 6(6):571-582.
14. Wu J, Wei W, Wang LY, Su ZG, Ma GH 2007. A thermosensitive hydrogel based on quaternized chitosan and poly(ethylene glycol) for nasal drug delivery system. Biomaterials 28(13):2220-2232.
15. Qian S, Wong YC, Zuo Z 2014. Development, characterization and application of in situ gel systems for intranasal delivery of tacrine. International journal of pharmaceutics 468(1-2):272-282.
16. Nazar H, Fatouros DG, van der Merwe SM, Bouropoulos N, Avgouropoulos G, Tsibouklis J, Roldo M 2011. Thermosensitive hydrogels for nasal drug delivery: the formulation and characterisation of systems based on N-trimethyl chitosan chloride. European journal of pharmaceutics and biopharmaceutics : official journal of Arbeitsgemeinschaft fur Pharmazeutische Verfahrenstechnik eV 77(2):225-232.
17. Li X, Kong X, Wang X, Shi S, Guo G, Luo F, Zhao X, Wei Y, Qian Z 2010. Gel-sol-gel thermo-gelation behavior study of chitosan-inorganic phosphate solutions. European journal of pharmaceutics and biopharmaceutics : official journal of Arbeitsgemeinschaft fur Pharmazeutische Verfahrenstechnik eV 75(3):388-392.
18. Li C, Li C, Liu Z, Li Q, Yan X, Liu Y, Lu W 2014. Enhancement in bioavailability of ketorolac tromethamine via intranasal in situ hydrogel based on poloxamer 407 and carrageenan. International journal of pharmaceutics 474(1-2):123-133.
19. Jeong B, Kim SW, Bae YH 2002. Thermosensitive sol-gel reversible hydrogels. Adv Drug Deliv Rev 54(1):37-51.

20. Chen X, Zhi F, Jia X, Zhang X, Ambardekar R, Meng Z, Paradkar AR, Hu Y, Yang Y 2013. Enhanced brain targeting of curcumin by intranasal administration of a thermosensitive poloxamer hydrogel. J Pharm Pharmacol 65(6):807-816.
21. Alsarra IA, Hamed AY, Mahrous GM, El Maghraby GM, Al-Robayan AA, Alanazi FK 2009. Mucoadhesive polymeric hydrogels for nasal delivery of acyclovir. Drug Dev Ind Pharm 35(3):352-362.
22. Agrawal AK, Gupta PN, Khanna A, Sharma RK, Chandrawanshi HK, Gupta N, Patil UK, Yadav SK 2010. Development and characterization of in situ gel system for nasal insulin delivery. Pharmazie 65(3):188-193.
23. Zaki NM, Awad GA, Mortada ND, Abd Elhady SS 2007. Enhanced bioavailability of metoclopramide HCl by intranasal administration of a mucoadhesive in situ gel with modulated rheological and mucociliary transport properties. European journal of pharmaceutical sciences : official journal of the European Federation for Pharmaceutical Sciences 32(4-5):296-307.
24. Nakamura K, Maitani Y, Lowman AM, Takayama K, Peppas NA, Nagai T 1999. Uptake and release of budesonide from mucoadhesive, pH-sensitive copolymers and their application to nasal delivery. J Control Release 61(3):329-335.
25. Ikechukwu Ugwoke M, Sam E, Van Den Mooter G, Verbeke N, Kinget R 1999. Nasal mucoadhesive delivery systems of the anti-parkinsonian drug, apomorphine: influence of drug-loading on in vitro and in vivo release in rabbits. International journal of pharmaceutics 181(1):125-138.
26. Hosny KM, Banjar ZM 2013. The formulation of a nasal nanoemulsion zaleplon in situ gel for the treatment of insomnia. Expert Opin Drug Deliv 10(8):1033-1041.
27. Basu S, Maity S 2012. Preparation and characterisation of mucoadhesive nasal gel of venlafaxine hydrochloride for treatment of anxiety disorders. Indian J Pharm Sci 74(5):428-433.
28. Zhou M, Donovan MD 1996. Intranasal mucociliary clearance of putative bioadhesive polymer gels. International journal of pharmaceutics 135(1–2):115-125.
29. Ugwoke MI, Exaud S, Van Den Mooter G, Verbeke N, Kinget R 1999. Bioavailability of apomorphine following intranasal administration of mucoadhesive drug delivery systems in rabbits. European journal of pharmaceutical sciences : official journal of the European Federation for Pharmaceutical Sciences 9(2):213-219.
30. Soane RJ, Hinchcliffe M, Davis SS, Illum L 2001. Clearance characteristics of chitosan based formulations in the sheep nasal cavity. International journal of pharmaceutics 217(1-2):183-191.
31. Luessen HL, de Leeuw BJ, Langemeyer MW, de Boer AB, Verhoef JC, Junginger HE 1996. Mucoadhesive polymers in peroral peptide drug delivery. VI. Carbomer and chitosan improve the intestinal absorption of the peptide drug buserelin in vivo. Pharmaceutical research 13(11):1668-1672.
32. Jain AK, Khar RK, Ahmed FJ, Diwan PV 2008. Effective insulin delivery using starch nanoparticles as a potential trans-nasal mucoadhesive carrier. European journal of pharmaceutics and biopharmaceutics : official journal of Arbeitsgemeinschaft fur Pharmazeutische Verfahrenstechnik eV 69(2):426-435.
33. Basu S, Bandyopadhyay AK 2010. Development and characterization of mucoadhesive in situ nasal gel of midazolam prepared with Ficus carica mucilage. AAPS PharmSciTech 11(3):1223-1231.
34. Kumar A, Garg T, Sarma GS, Rath G, Goyal AK 2015. Optimization of combinational intranasal drug delivery system for the management of migraine by using statistical design. European journal of pharmaceutical sciences : official journal of the European Federation for Pharmaceutical Sciences 70:140-151.
35. Ibrahim HK, Abdel Malak NS, Abdel Halim SA 2015. Formulation of Convenient, Easily Scalable, and Efficient Granisetron HCl Intranasal Droppable Gels. Mol Pharm 12(6):2019-2025.
36. Hosny KM, Hassan AH 2014. Intranasal in situ gel loaded with saquinavir mesylate nanosized microemulsion: preparation, characterization, and in vivo evaluation. International journal of pharmaceutics 475(1-2):191-197.
37. Pisal PB, Patil SS, Pokharkar VB 2013. Rheological investigation and its correlation with permeability coefficient of drug loaded carbopol gel: influence of absorption enhancers. Drug Dev Ind Pharm 39(4):593-599.
38. Chen E, Chen J, Cao SL, Zhang QZ, Jiang XG 2010. Preparation of nasal temperature-sensitive in situ gel of Radix Bupleuri and evaluation of the febrile response mechanism. Drug Dev Ind Pharm 36(4):490-496.
39. Callens C, Ceulemans J, Ludwig A, Foreman P, Remon JP 2003. Rheological study on mucoadhesivity of some nasal powder formulations. European journal of pharmaceutics and biopharmaceutics : official journal of Arbeitsgemeinschaft fur Pharmazeutische Verfahrenstechnik eV 55(3):323-328.

40. Narola B, Singh AS, Santhakumar PR, Chandrashekhar TG 2010. A Validated Stability-indicating Reverse Phase HPLC Assay Method for the Determination of Memantine Hydrochloride Drug Substance with UV-Detection Using Precolumn Derivatization Technique. Analytical chemistry insights 5:37-45.
41. Associations IFoPM. 1996. Validation of analytical procedures: text and methodology. Proceedings of the International Conference on Harmonization, Methodology Q2(R1) ed., Geneva, Switzerland: International Conference on Harmonisation.
42. Varshosaz J, Sadrai H, Heidari A 2006. Nasal delivery of insulin using bioadhesive chitosan gels. Drug delivery 13(1):31-38.
43. Chi SC, Jun HW 1991. Release rates of ketoprofen from poloxamer gels in a membraneless diffusion cell. Journal of pharmaceutical sciences 80(3):280-283.
44. Martinac A, Filipovic-Grcic J, Voinovich D, Perissutti B, Franceschinis E 2005. Development and bioadhesive properties of chitosan-ethylcellulose microspheres for nasal delivery. International journal of pharmaceutics 291(1-2):69-77.
45. Korsmeyer R, Gurny, R., Doelker, E., Buri, B., Peppas, N.A. 1983. Mechanisms of solute release from porous hydrophilic polymers. International journal of pharmaceutics 15(1):25-35.
46. Siepmann J, Peppas NA 2001. Modeling of drug release from delivery systems based on hydroxypropyl methylcellulose (HPMC). Adv Drug Deliv Rev 48(2-3):139-157.
47. Kim H, Fassihi R 1997. A new ternary polymeric matrix system for controlled drug delivery of highly soluble drugs: I. Diltiazem hydrochloride. Pharmaceutical research 14(10):1415-1421.
48. Bettini R, Colombo P, Massimo G, Catellani PL, Vitali T 1994. Swelling and drug release in hydrogel matrices: polymer viscosity and matrix porosity effects. European Journal of Pharmaceutical Sciences 2(3):213-219.
49. Peppas NA, Sahlin JJ 1989. A simple equation for the description of solute release. III. Coupling of diffusion and relaxation. International journal of pharmaceutics 57(2):169-172.
50. Reichl S, Becker K 2012. Cultivation of RPMI 2650 cells as an in-vitro model for human transmucosal nasal drug absorption studies: optimization of selected culture conditions. Journal of Pharmacy and Pharmacology 64(11):1621-1630.
51. Reichl S, Becker K 2012. Cultivation of RPMI 2650 cells as an in-vitro model for human transmucosal nasal drug absorption studies: optimization of selected culture conditions. The Journal of pharmacy and pharmacology 64(11):1621-1630.
52. Bai S, Yang T, Abbruscato TJ, Ahsan F 2008. Evaluation of human nasal RPMI 2650 cells grown at an air-liquid interface as a model for nasal drug transport studies. Journal of pharmaceutical sciences 97(3):1165-1178.
53. Kundoor V, Dalby RN 2010. Assessment of nasal spray deposition pattern in a silicone human nose model using a color-based method. Pharmaceutical research 27(1):30-36.
54. Cho HJ, Balakrishnan P, Park EK, Song KW, Hong SS, Jang TY, Kim KS, Chung SJ, Shim CK, Kim DD 2011. Poloxamer/cyclodextrin/chitosan-based thermoreversible gel for intranasal delivery of fexofenadine hydrochloride. Journal of pharmaceutical sciences 100(2):681-691.
55. Almdal K, Dyre J, Hvidt S, Kramer O 1993. Towards a phenomenological definition of the term 'gel'. Polymer Gels and Networks 1(1):5-17.
56. Islam MT, Rodriguez-Hornedo N, Ciotti S, Ackermann C 2004. Rheological characterization of topical carbomer gels neutralized to different pH. Pharmaceutical research 21(7):1192-1199.
57. Kabanov AV, Batrakova EV, Alakhov VY 2002. Pluronic block copolymers as novel polymer therapeutics for drug and gene delivery. Abstr Pap Am Chem S 223:U438-U438.
58. Pisal SS, Paradkar AR, Mahadik KR, Kadam SS 2004. Pluronic gels for nasal delivery of Vitamin B12. Part I: preformulation study. Int J Pharm 270(1-2):37-45.
59. Good W 1983. Transder®-Nitro Controlled Delivery of Nitroglycerin via the Transdermal Route. Drug Development and Industrial Pharmacy 9(4):647-670.
60. Henriksen I, Green KL, Smart JD, Smistad G, Karlsen J 1996. Bioadhesion of hydrated chitosans: An in vitro and in vivo study. International journal of pharmaceutics 145(1–2):231-240.
61. Khutoryanskiy VV 2011. Advances in mucoadhesion and mucoadhesive polymers. Macromolecular bioscience 11(6):748-764.

62. J C. 1967. The mathematics of diffusion. ed., Oxford: Clarendon Press.
63. Lin WC, Yu DG, Yang MC 2005. pH-sensitive polyelectrolyte complex gel microspheres composed of chitosan/sodium tripolyphosphate/dextran sulfate: swelling kinetics and drug delivery properties. Colloids and surfaces B, Biointerfaces 44(2-3):143-151.
64. Khare AR, Peppas NA 1995. Swelling/deswelling of anionic copolymer gels. Biomaterials 16(7):559-567.
65. Klech CMS, A.P. 1989. Examination of the moving boundaries associated with non-fickian water swelling of glassy gelatin beads: Effect of solution pH. Journal of Membrane Science 43:87-101.
66. De Kee D, Liu Q, Hinestroza J 2005. Viscoelastic (Non-Fickian) Diffusion. The Canadian Journal of Chemical Engineering 83(6):913-929.
67. Vrentas JS, Vrentas CM 1998. Integral sorption in glassy polymers. Chemical Engineering Science 53(4):629-638.
68. Aminabhavi TM, Aithal US, Shukla SS 1989. Molecular transport of organic liquids through polymer films. Journal of Macromolecular Science, Part C 29(2-3):319-363.
69. Wu JC, Peppas NA 1993. Modeling of penetrant diffusion in glassy polymers with an integral sorption deborah number. Journal of Polymer Science Part B: Polymer Physics 31(11):1503-1518.
70. Thomas NL, Windle AH 1982. A theory of case II diffusion. Polymer 23(4):529-542.
71. Thomas NL, Windle AH 1981. Diffusion mechanics of the system PMMA-methanol. Polymer 22(5):627-639.
72. Thomas NL, Windle AH 1980. A deformation model for Case II diffusion. Polymer 21(6):613-619.
73. Crank JP, G.S. 1968. Diffusion in polymers. ed., London: Academic Press.
74. HJ F. 1966. Irreversible Thermodynamics of Internally Relaxing Systems in the Vicinity of the Glass Transition. In Dennelly RJ HRaPI, editor Non-Equilibrium Thermodynamics, Variational Techniques, and Stability, ed.: University of Chicago Press. p 277-280.
75. Long FA, Richman D 1960. Concentration Gradients for Diffusion of Vapors in Glassy Polymers and their Relation to Time Dependent Diffusion Phenomena1,2. Journal of the American Chemical Society 82(3):513-519.
76. Alfrey T, Gurnee EF, Lloyd WG 1966. Diffusion in glassy polymers. Journal of Polymer Science Part C: Polymer Symposia 12(1):249-261.
77. Orienti I, Gianasi, E., Zecchi, V., Conte, U. 1995. Release of ketoprofen from microspheres of poly2-hydroxyethyl methacrylate or poly2-hydroxyethyl methacrylate-cob- methacryloyloxyethyl deoxycholate crosslinked with ethylene glycol dimethacrylate and tetraethylene glycol dimethacrylate. European Journal of Pharmaceutics and Biopharmaceutics 41:247-253.
78. Davidson GWR, Peppas, P. 1986. Solute and water diffusion in swellable copolymers versus relaxation controlled transport in phema-co-mma copolymers. Journal of Controlled Release 3:243-258.
79. Franson NM, Peppas NA 1983. Influence of copolymer composition on non-fickian water transport through glassy copolymers. Journal of Applied Polymer Science 28(4):1299-1310.
80. Hopfenberg H. 1974. Super case II transport of organic vapors in glassy polymers. In HB H, editor Permeability of plastic films and coatings to gases, vapors, and liquids, ed., New York: Plenum Press.
81. Peppas NA, Khare AR 1993. Preparation, structure and diffusional behavior of hydrogels in controlled release. Advanced Drug Delivery Reviews 11(1–2):1-35.
82. Stuart BO 1973. Deposition of inhaled aerosols. Archives of internal medicine 131(1):60-73.
83. Hatch TF 1961. Distribution and deposition of inhaled particles in respiratory tract. Bacteriological reviews 25:237-240.
84. Hatch TF 1961. Distribution and deposition of the inhaled particles in respiratory tract. Bacteriological reviews 25:237-240.
85. Gross EA, Swenberg JA, Fields S, Popp JA 1982. Comparative morphometry of the nasal cavity in rats and mice. J Anat 135(Pt 1):83-88.
86. Badhan RK, Kaur M, Lungare S, Obuobi S 2014. Improving brain drug targeting through exploitation of the nose-to-brain route: a physiological and pharmacokinetic perspective. Curr Drug Deliv 11(4):458-471.
87. Kundoor V, Dalby RN 2011. Effect of formulation- and administration-related variables on deposition pattern of nasal spray pumps evaluated using a nasal cast. Pharmaceutical research 28(8):1895-1904.

88. Guo Y, Laube B, Dalby R 2005. The effect of formulation variables and breathing patterns on the site of nasal deposition in an anatomically correct model. Pharmaceutical research 22(11):1871-1878.

List of Figures

Figure 1: Rheological analysis of AMT containing thermoresponsive gels containing FCS, FPEG or FCMC. (A): Temperature sweep analyses; (B) Time-sweep analyses (fixed at 34 °C).

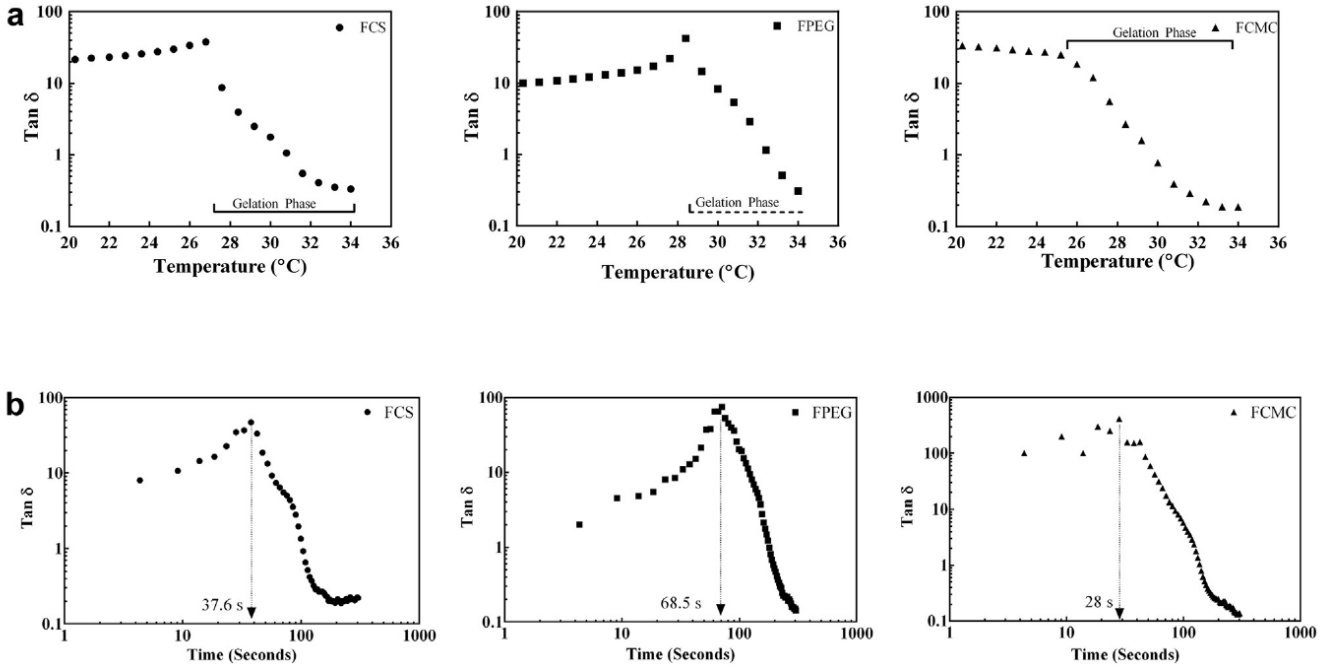

Figure 2: Shear viscosity analysis of the formulations at ambient (18 °C) and nasal cavity (34 °C) temperature.

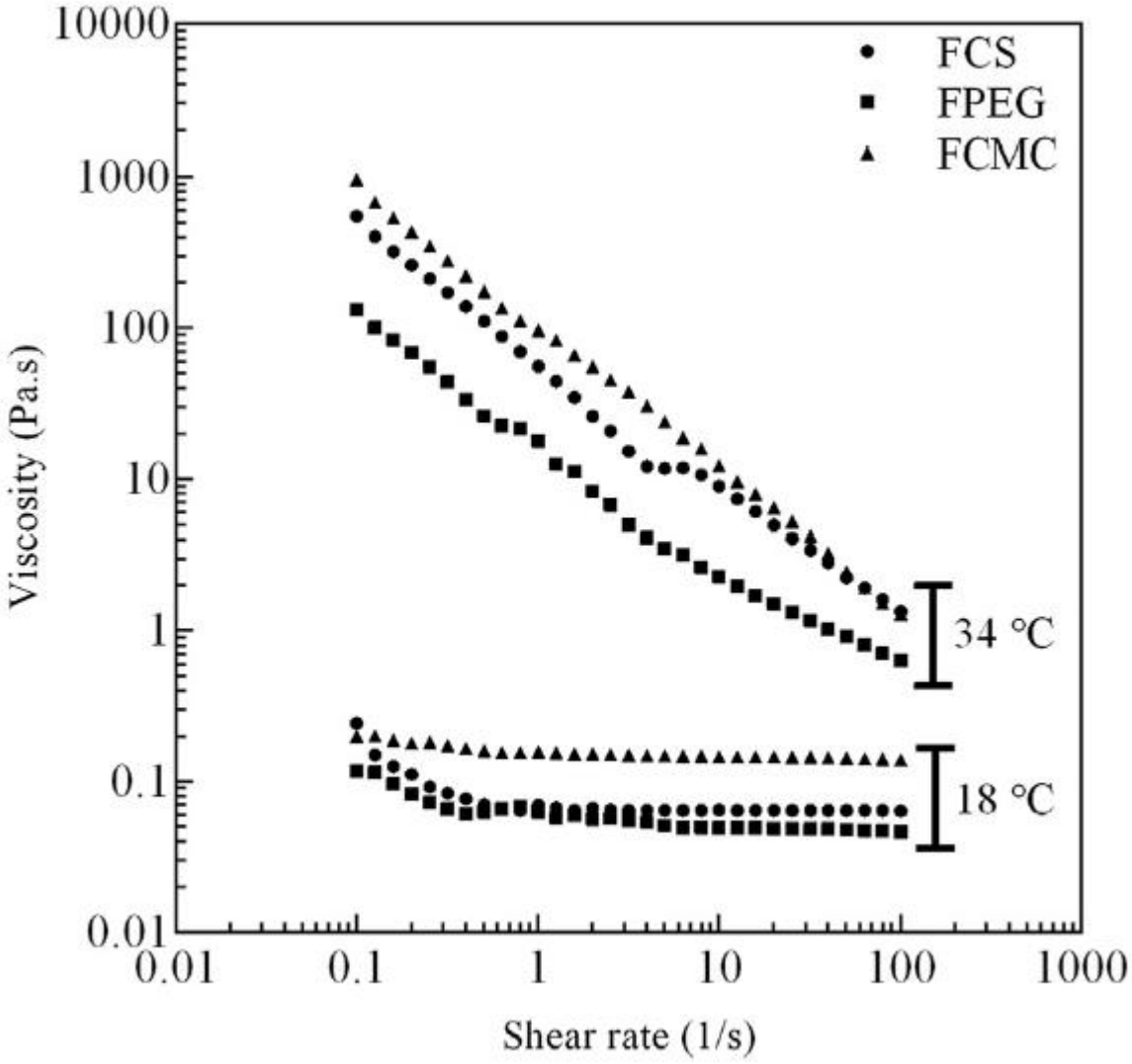

Figure 3: Drip transfer of optimised formulations in the presence and absence of mucin-containing agar gel plates include at 45° to the plane and maintained at 34 °C. *** p < P 0.001.

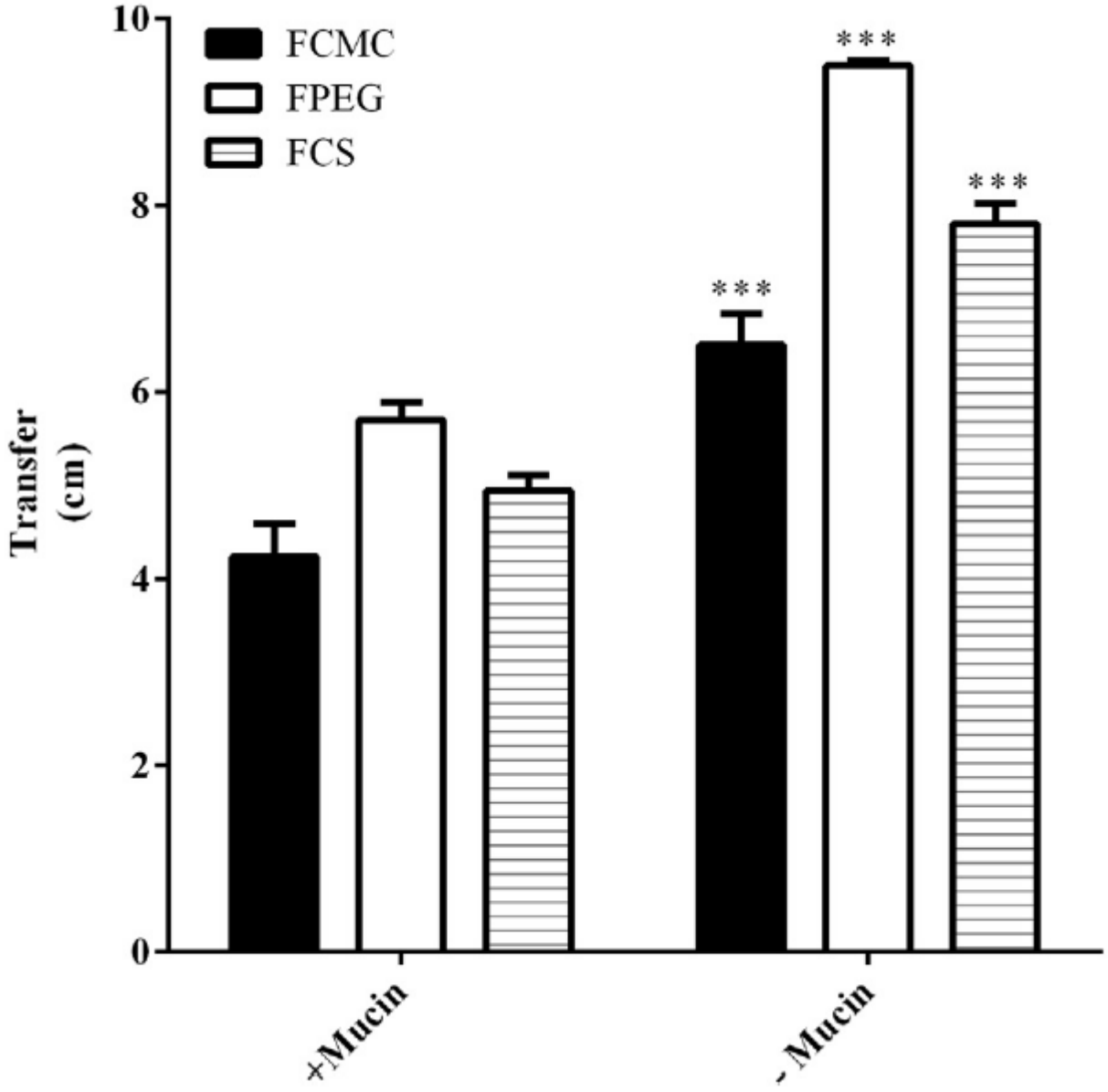

Figure 4: Amantadine cumulative % release for optimised formulations following storage at 4°C and 25°C for up to 8 weeks. (A) Cumulative % AMT release for samples successfully gelling at nasal cavity temperature (34 °C); (B) Comparison of AMT release from FCMC and FCS at preparation (Week 0) and at the end of the stability period (Week 8). * $p < 0.05$, ** $p < 0.01$.

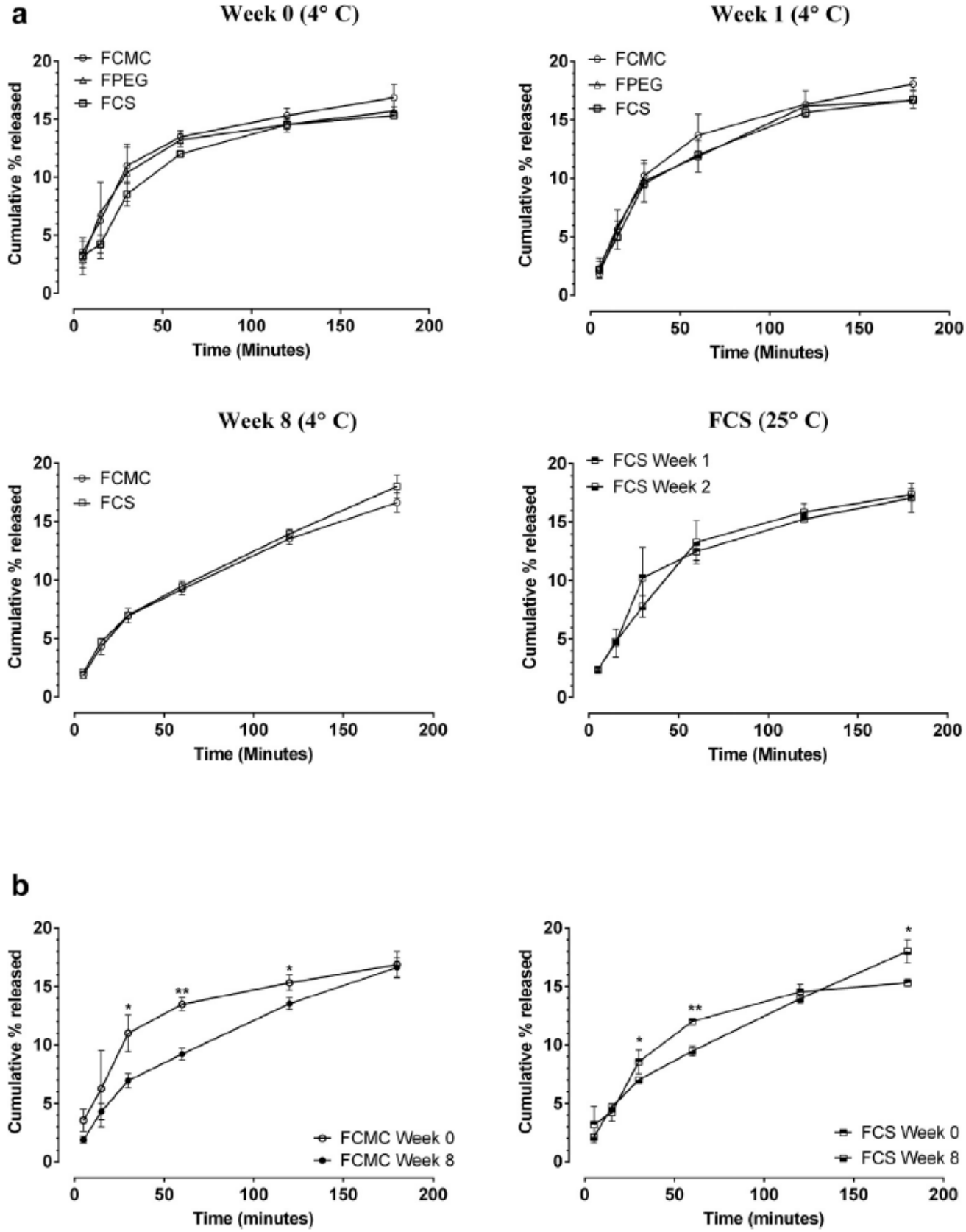

Figure 5: Cellular toxicity of amantadine, CMC, PEG4000 and F127 on RPMI 2650 cells. Cells were grown on a 96-well plate and exposed to various concentrations of amantadine (0. 1 nM – 10 mM) or polymer (10-4,000 µg/mL) for 24 hours. Data is reported as mean ± SD with up to 8 replicates per compound in at least 3 independent experiments.

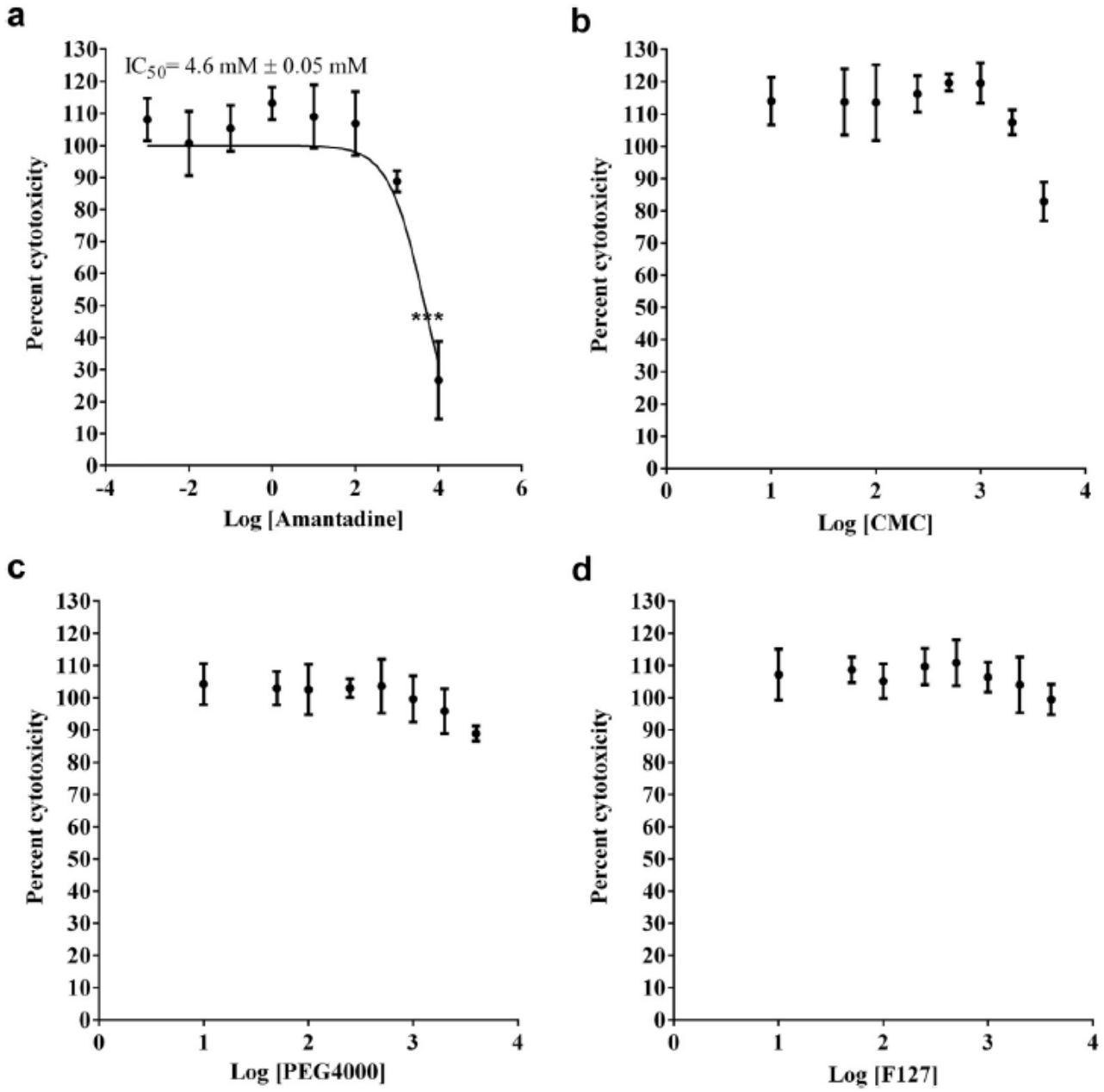

Figure 6: Transport of AMT across an *in vitro* cell culture model of the nasal epithelial, from optimised formulations in HBSS-HEPES transport media. ** $p < 0.01$.

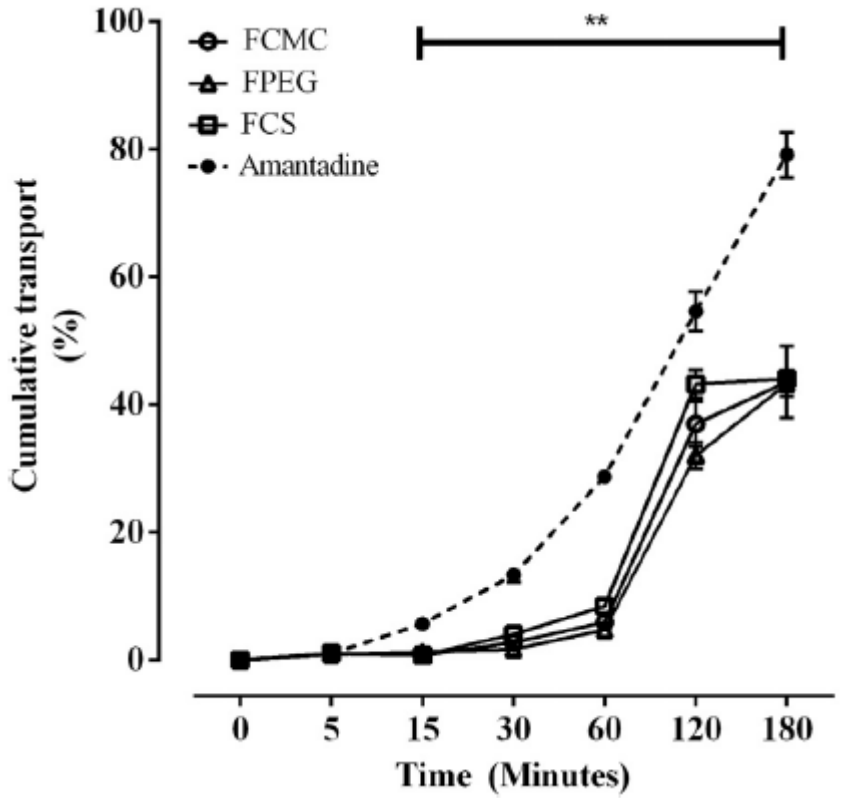

Figure 7: Representative nasal deposition patterns of FCMC. Brown colours represent the applied Kolor-Kut and green colours resent the depositions patterns of the spray. Angles refer to nasal spray position relative to the horizontal place (60, 70 or 80°), insertion of the spray orifice into the nostril (5 mm) or with the nasal cast angled 15° forward.

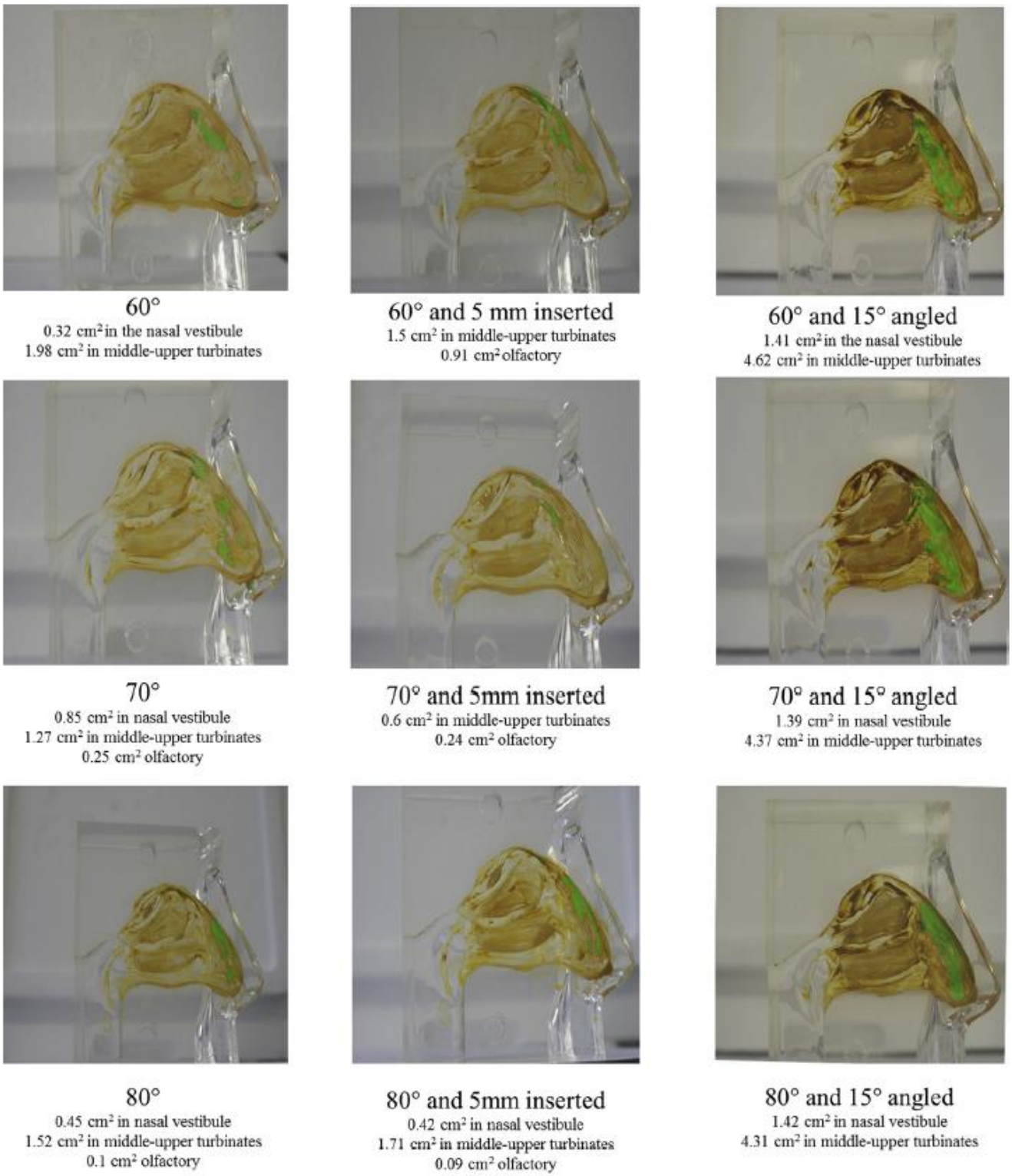

Figure 8: Representative nasal deposition patterns of FCS. Brown colours represent the applied Kolor-Kut and green colours resent the depositions patterns of the spray. Angles refer to nasal spray position relative to the horizontal place (60, 70 or 80°), insertion of the spray orifice into the nostril (5 mm) or with the nasal cast angled 15° forward.

60°
0.52 cm^2 in the nasal vestibule
3.02 cm^2 in middle-upper turbinates
0.7 cm^2 olfactory

60° and 5 mm inserted
1 cm^2 in the nasal vestibule
0.9 cm^2 in middle-upper turbinates
0.6 cm^2 olfactory

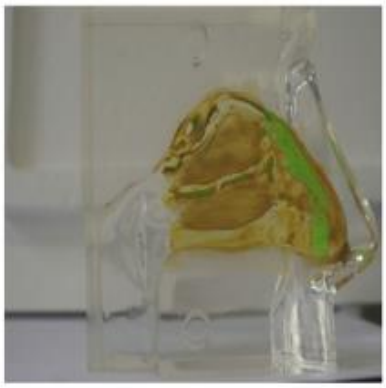

60° and 15° angled
1.41 cm^2 in the nasal vestibule
4.56 cm^2 in middle-upper turbinates
0.2 cm^2 olfactory

70°
0.65 cm^2 in nasal vestibule
2.17 cm^2 in middle-upper turbinates
0.28 cm^2 olfactory

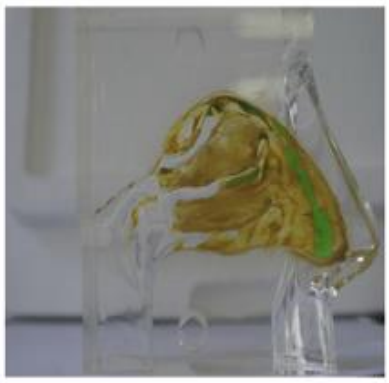

70° and 5mm inserted
1.02 cm^2 in nasal vestibule
2.35 cm^2 in middle-upper turbinates
0.3 cm^2 olfactory

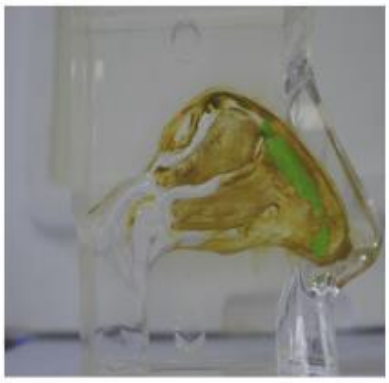

70° and 15° angled
1.1 cm^2 in nasal vestibule
4.37 cm^2 in middle-upper turbinates

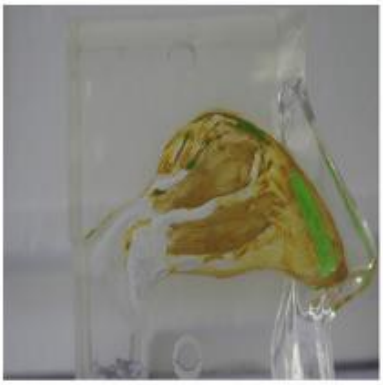

80°
0.91 cm^2 in nasal vestibule
3.01 cm^2 in middle-upper turbinates
0.5 cm^2 olfactory

80° and 5mm inserted
1.42 cm^2 in nasal vestibule
3.7 cm^2 in middle-upper turbinates
0.15 cm^2 olfactory

80° and 15° angled
1.35 cm^2 in nasal vestibule
4.05 cm^2 in middle-upper turbinates
0.4 cm^2 olfactory

List of Tables

Table 1: Power law rheological analysis of amantadine containing thermoresponsive nasal gels

Formulation	**Temperature** (°C)	***k***	***n***	**Behaviour**
FCMC	18	0.157	0.972	Newtonian
FPEG	18	0.0545	0.971	Newtonian
FCS	18	0.0656	1	Newtonian
FCMC	34	100.2	0.066	Non-Newtonian
FPEG	34	13.59	0.3043	Non-Newtonian
FCS	34	56.56	0.1762	Non-Newtonian

Table 2: Drug release kinetics analysis of formulations stored at ambient (18 °C) and nasal cavity (34 °C) temperature for up to 8 weeks.

	Week	Formulation	Korsmeyer-Peppas
4 °C	0	FCMC	*kKP* = 2.859 ± 0.899 ; n =0.391 ± 0.051
		FPEG	*kKP* = 2.931 ± 1.160 ; n =0.352 ± 0.076
		FCS	*kKP* = 2.888 ± 0.632 ; n =0.684 ± 0.039
	1	FCMC	*kKP* = 2.004 ± 0.027 ; n =0.438 ± 0.024
		FPEG	*kKP* = 2.012 ± 0.032 ; n =0.423 ± 0.013
		FCS	*kKP* = 1.852 ± 0.135 ; n =0.433 ± 0.019
	8	FCMC	*kKP* = 1.034 ± 0.170 ; n =0.538 ± 0.024
		FCS	*kKP* = 1.011 ± 0.092 ; n =0.553 ± 0.024
25 °C	1	FCS	*kKP* = 1.997 ± 0.659 ; n =0.433 ± 0.059
	2	FCS	*kKP* = 1.614 ± 0.351 ; n =0.474 ± 0.042

kKP: Korsmeyer-Peppas constant; *n*= release exponent. Mean ± SD**.**

Table 3. Laser diffraction particle size analysis

	Diameter (µm)				
	Dv10	Dv50	Dv90	VMD	Span
FCS	7.27 ± 0.28	109.07 ± 3.42	157.77 ± 0.99	92.41 ± 1.72	1.38 ± 0.21
FCMC	39.81 ± 1.02	129.86 ± 0.29	167.39 ± 0.09	120.87 ± 0.59	0.98 ± 0.30
FPEG	43.93 ± 0.88	104.67 ± 1.88	150.95 ± 1.04	100.35 ± 1.53	1.02 ± 0.06

Mean ±SD, 6 replicate spray actuations *per* formulation.

Dv10: 10 % of the cumulative undersized (volume) fraction; Dv50: 50 % of the cumulative undersized (volume) fraction; Dv90: 90 % of the cumulative undersized (volume) fraction; VMD: volume mean diameter; Span: relative span (Dv90-Dv10)/Dv50.